Scientia Iranica, Vol. 13, No. 1, pp 60 66

SCIENTIA IRANICA

Design and Simulation of an Oblique Suspender MEMS Variable Capacitor

H. Nabovati*, K. Mafinezhad[1], H. Keshmiri[1] and A. Nabovati[2]

This paper presents the results on the development of a novel micromachined parallel plate tunable capacitor with a wide tuning range. Different from conventional parallel plate capacitors, this novel tunable capacitor consists of one suspended top plate, suspending with four oblique arms and one bottom fixed plate. These oblique arms increase the length of the cantilevers, in order to cause more deflection and, hence, increase the tuning range of the capacitor for constant bias voltage. Applying a DC voltage between two plates provides electrostatic actuation for capacitance tuning. According to electromagnetic simulation, a tuning range of 146% has been achieved with a 1.7 volt bias voltage. An empirical behavioral model is extracted from simulated y parameters of the structure.

INTRODUCTION

The increasing demand for smaller and more capable portable phones, notebook computers, global positioning system receivers and remote sensors, has spawned an explosive growth in wireless technology. As the demand increases, more efficient use of an allocated spectral frequency range and much more capable implantation technologies are required. In recent years, MEMS (Micro Electromechanical Systems) technology has begun to be used in wireless communication systems, to improve the performance of existing devices based on structures or operational principles.

At present, the ultimate miniaturization of super heterodyne transceivers is limited mainly by the need for numerous off-chip frequency selective passive components, such as variable capacitors and inductors. A variable capacitor is the basic component of a Voltage Controlled Oscillator (VCO) used in frequency synthesizers, which generates the local oscillator signals. Currently, such VCO's are implemented using off-chip inductors (with a Q of at least 30) combined with off-chip voltage tunable varactor diodes (with a Q of at least 40). Recent demonstrations of voltage tunable capacitors comprised of micromachined, movable metal plates, now offer substantial improvements over varactor diodes. Compared with solid state varactors, micromachined variable capacitors have the advantage of lower loss, a higher quality factor and potentially greater tuning range [1-4].

The recent applications of MEMS technologies in voltage tunable capacitors use two methods, the electrothermal method and electrostatic method. The electrothermal method uses the deflection of supporting arms, due to the different axial strain of a compound beam when a temperature difference is exerted. This method has a wide tuning range, but is slow and needs more space. In the electrostatic method, capacitance is tuned by varying the distance between two plates using an electrostatic force caused by a bias voltage. The desired capacitance is accomplished by fast tuning and small space, but, the theoretical tuning range is limited by 150% [5]. Among all the MEMS tunable capacitors developed before, the parallel plate configuration with electrostatic actuation is the most commonly used [4,5]. The main effort applied in designing these structures is in developing tunability and decreasing the structure loss that will lead to a higher quality factor.

In the present work, the development of a novel MEMS electrostatically tunable capacitor has been studied using full wave electromagnetic simulation. This new design keeps the simplicity of conventional two parallel plate configurations, while providing a much wider tuning range. An empirical behavioral model is extracted that can be defined by circuit

*. *Corresponding Author, Department of Electrical Engineering, Ferdowsi University of Mashhad, Mashhad, I.R. Iran.*

1. *Department of Electrical Engineering, Ferdowsi University of Mashhad, Mashhad, I.R. Iran.*
2. *Department of Mechanical Engineering, University of New Brunswick, Canada.*

simulator software and can be scaled according to device dimensions.

The new tunable capacitor can be fabricated using a standard surface micromachined process and can be monolithically integrated with other RF circuits.

MECHANICAL DESIGN

As schematically shown in Figure 1, the top plate of the capacitor has been suspended using four oblique cantilever beams. Using the basic mechanics been suspended using four oblique cantilever beams. Using the basic mechanics of solids, it can be shown that the deflection of a cantilever beam, which has been subjected to a concentrated load at its end, can be calculated as below [6]:

$$\delta = \frac{Fl^3}{3YI}, \tag{1}$$

in which F, l, I and Y are applied force, beam length, moment of inertia of beam cross section and Young's modulus of elasticity, respectively. It means that the deflection is a cubic function of beam length, so, this novel design using oblique beams, takes advantage of this property and produces a 283% increase in the deflection of the beams, in comparison with conventional normal beams. It means that a lower bias voltage is needed for a constant tuning range of the capacitor.

When a DC bias voltage is applied between two plates, with an initial gap size of 1.2 μm at $V = 0$, an attractive electrostatic force is generated between them and the top plate moves toward the fixed one, until equilibrium between electrostatic and mechanical forces is achieved. By neglecting the firing effect, the capacitance of the capacitor, which has been formed between the two plates, can be written as:

$$C = \varepsilon \frac{A}{x}, \tag{2}$$

where x is the distance between two plates, A is the plate surface area and ε is the permittivity of the air gap. When the bias voltage, V, is applied, the stored electrical energy will be:

$$E = \frac{1}{2}CV^2 = \frac{\varepsilon AV^2}{2x}. \tag{3}$$

Assuming a potential field, the electrostatic force between two plates can be calculated as:

$$F = \frac{\partial E}{\partial x}, \tag{4}$$

in which x is the distance between two plates and is equal to $x_0 \quad \delta$ and where δ is the deflection of the beams. The mechanical force exerted on the top plate, due to the deflection of the four beams, can be calculated using the following equation:

$$F = 12\frac{EI\delta}{l^3} = 12\frac{EI(x_0 \quad x)}{l^3}, \tag{5}$$

where E is the Young's module, l is the arm length, x_0 is the initial distance and I is the moment of inertia for the cantilever beam, which could be calculated according to the following equation;

$$I = \frac{wt^3}{3}, \tag{6}$$

in which w is the beam width and t stands for its thickness. When the equilibrium between electrostatic and mechanical forces is achieved, the top plate will be in force equilibrium, thus;

$$\frac{12EI(x_0 \quad x)}{l^3} = \frac{\varepsilon AV^2}{2x^2}. \tag{7}$$

It is important to note that the corresponding value of V at $x = 2/3x_0$ is the critical point and is called the pull-in voltage [5]. If V is increased beyond this value, no equilibrium can be achieved and the top plate will move toward the bottom one until they snap into contact. This phenomenon is called the pull-in effect. Thus, according to Equation 6, theoretically, the maximum capacitance of the variable capacitor is 150% of its initial value at $V = 0$.

Figure 2 shows the distance of two plates versus the applied bias voltage. The effect of an oblique beam in increasing the deflection is vividly obvious. The initial distance is assumed as 1.2 μm and the pull-in effect has occurred at 1.7 V for the oblique beams. At this point, the distance between two plates reaches 0.8 μm.

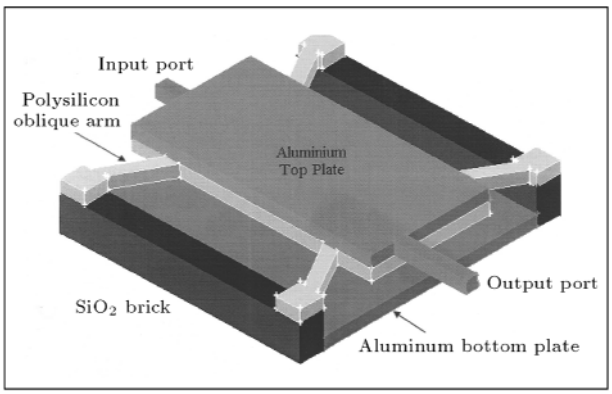

Figure 1. Perspective of the designed structure.

ELECTROMAGNETIC SIMULATION

The full wave electromagnetic simulation of the capacitor has been done using MEM Research EM3DS 6.1 [7,8]. In the simulation, a box with the size of

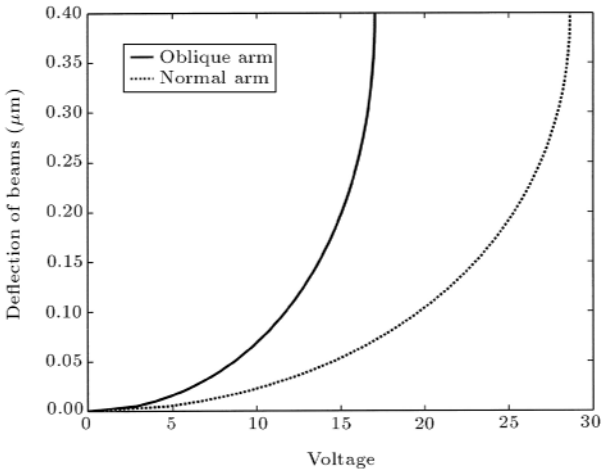

Figure 2. Variation of gap distance verses bias voltage $L = 42$ μm, $t = 0.5$ μm, $w = 7$ μm, $A = 200 \times 200$ μm^2.

400×400 μm is used. The top wall of the structure is assumed to be infinity dielectric and the bottom wall is a perfect conductor.

After a full wave analysis, y parameters of the structure are extracted in the frequency range from 1 GHz to 5 GHz for different distances between the capacitor plates. Figures 3 and 4 represent simulation results for y_{11} and y_{22} when the distances are equal to 0.6, 1 and 1.6 μm, respectively.

The structure, as schematically shown in Figure 5, consists of 6 different layers. The substrate is assumed to be lossy silicon with a relative dielectric constant of 11.8 and a conductivity of 0.0033S/m. The thickness of this layer is 1000 μm.

The substrate is assumed to be coated with 1.5 μm thick dielectric with a relative dielectric constant of 7.6 (corresponding to silicon nitride).

The capacitor bottom plate is realized with 0.5 μm thick aluminum with a resistivity of 3×10^{-8} Ωm, which is deposited on the dielectric layer. The top plate is suspended using two dielectric bricks with a relative dielectric constant of 3.9 (corresponding to silicon dioxide). The top layer of the variable capacitor consists of two layers. The first one, which is suspended by cantilever arms, is assumed to be polysilicon with a 0.5 μm thickness and a resistivity of 3×10^{-5} Ωm. The next layer has been embedded over the polysilicon layer and is assumed to be aluminum with a thickness of 0.5 μm.

The complete structure is schematically shown in Figure 1. The results of the electromagnetic simulation are used to extract an equivalent circuit model for the voltage tunable capacitor. Moreover, the quality

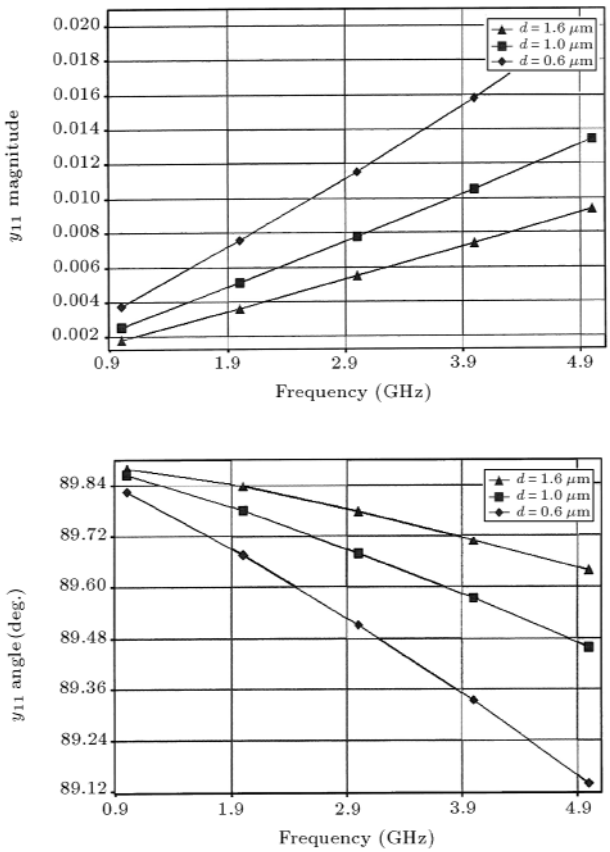

Figure 3. Magnitude and angle of y_{11} for variable gap distances (0.6, 1 and 1.6 μm).

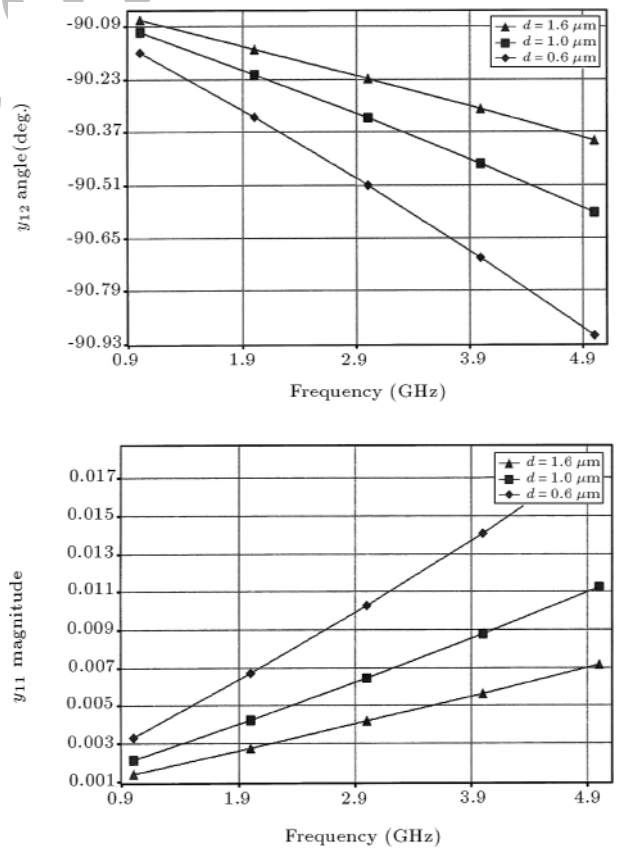

Figure 4. Magnitude and angle of y_{12} for variable gap distances (0.6, 1 and 1.6 μm).

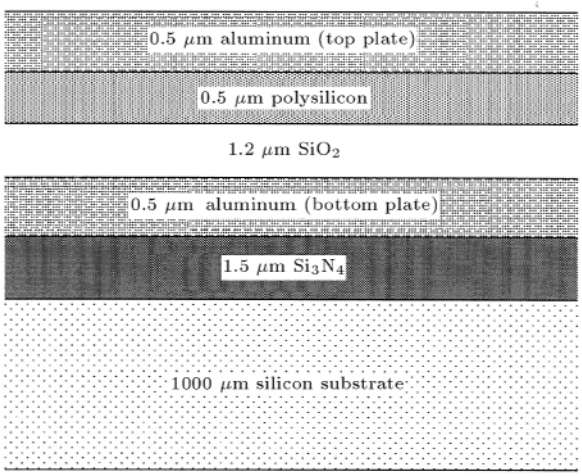

Figure 5. Cross section of the structure.

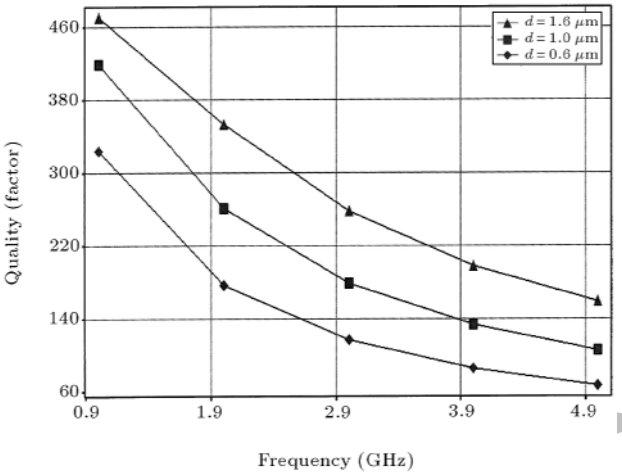

Figure 6. Quality factor for variable gap distances (0.6, 1 and 1.6 μm).

factor and current density of MEMS have been calculated.

Figure 6 shows, respectively, the EM simulated quality factor of the structure with gaps of 0.6, 1 and 1.6 μm between the two plates. The quality factor exceeds 460 in 1GHz, which is sufficient for almost every communication application.

Figure 7 presents the current density distribution over the surface of the top and bottom plates. For this simulation, the input and output ports have been terminated with short circuits and the calculation was done in 3GHz. The calculation was done when the input port was stimulated with a 1-volt signal.

EMPIRICAL BEHAVIORAL MODELING

Figure 8 presents an equivalent circuit model for a variable MIM capacitor. The network has been selected for accurate broadband modeling of the structure.

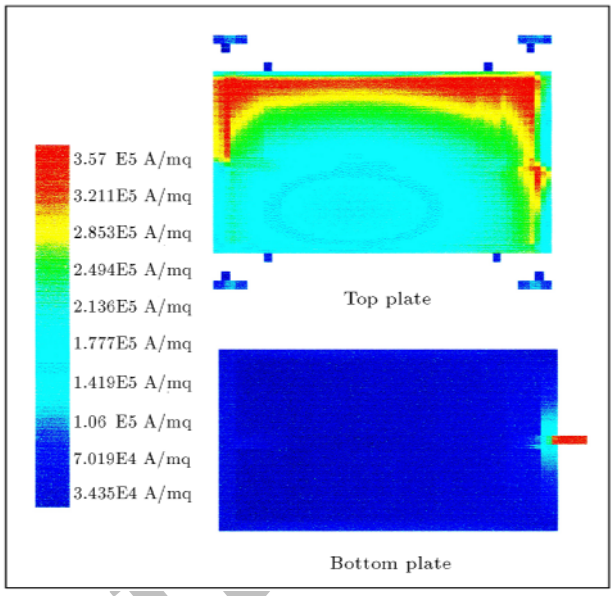

Figure 7. Current density contour in two plates.

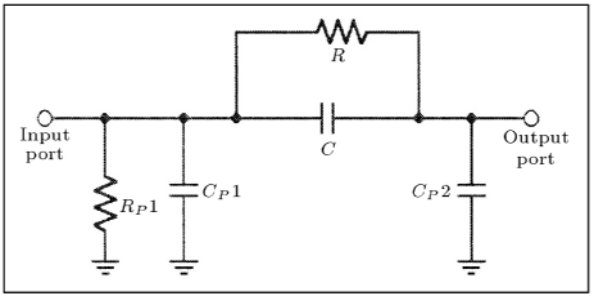

Figure 8. Equivalent circuit for designed variable capacitor.

In this circuit, C models the capacitance between two ports and R stands for capacitance leakage. These two parameters present an intrinsic model of the MEMS.

Three parasitic elements present the capacitance extrinsic model of the MEMS. C_{p1} and C_{p2} model the parasitic capacitance of the structure and R_{p1} corresponds to the power dissipation at the input port. The output dissipation is negligible.

Using the results of full wave analyses, for different distances between the plates, the equivalent circuit parameters are extracted and scaled according to the distance. The y parameters are used for this purpose. The procedure is straightforward and has been presented in Equations 7 to 11;

$$R = \frac{1}{\mathrm{Re}(y_{12})}, \tag{8}$$

$$C = \frac{\mathrm{Im}(y_{12})}{2\pi f}, \tag{9}$$

$$R_{P1} = \frac{1}{\mathrm{Re}(y_{11}) \quad \frac{1}{R}}, \tag{10}$$

$$C_{P1} = \frac{\mathrm{Im}(y_{11})}{2\pi f} \quad C, \tag{11}$$

$$C_{P2} = \frac{\mathrm{Im}(y_{22})}{2\pi f} \quad C. \tag{12}$$

The results are summarized in Figures 9 to 12 and the values of the intrinsic and parasitic elements of the equivalent circuit are reported for various device dimensions. It is obvious that the variation of parasitic capacitance according to gap distance is almost negligible. The thickness and permittivity of the substrate coating layer and substrate conductance are the most important parameters, which control parasitic capacitances.

According to these calculations, a behavioral intrinsic model is extracted, which defines these elements as a function of gap distance.

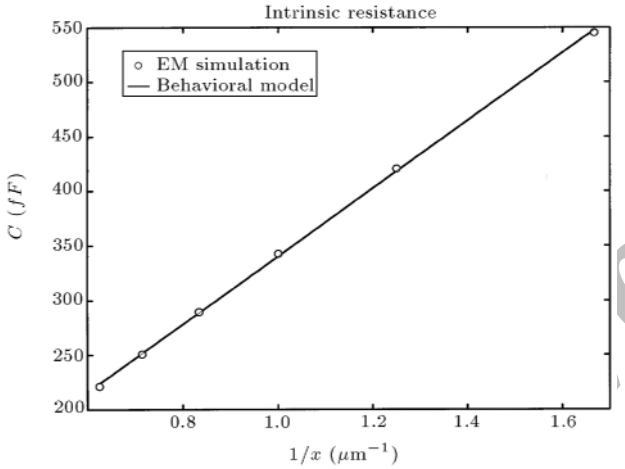

Figure 9. Modeled and simulated values of intrinsic capacitance.

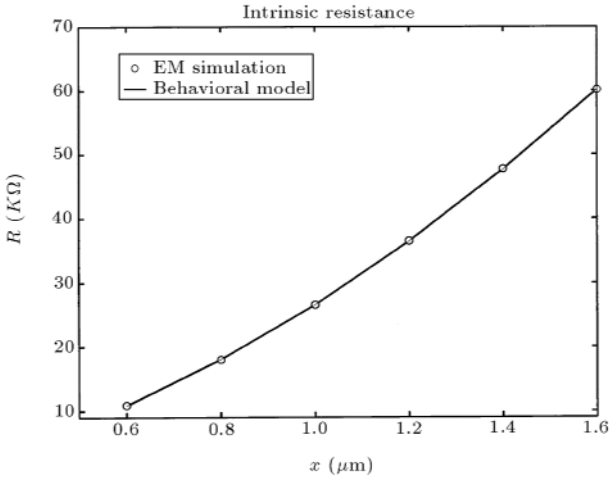

Figure 10. Modeled and simulated values of intrinsic resistance.

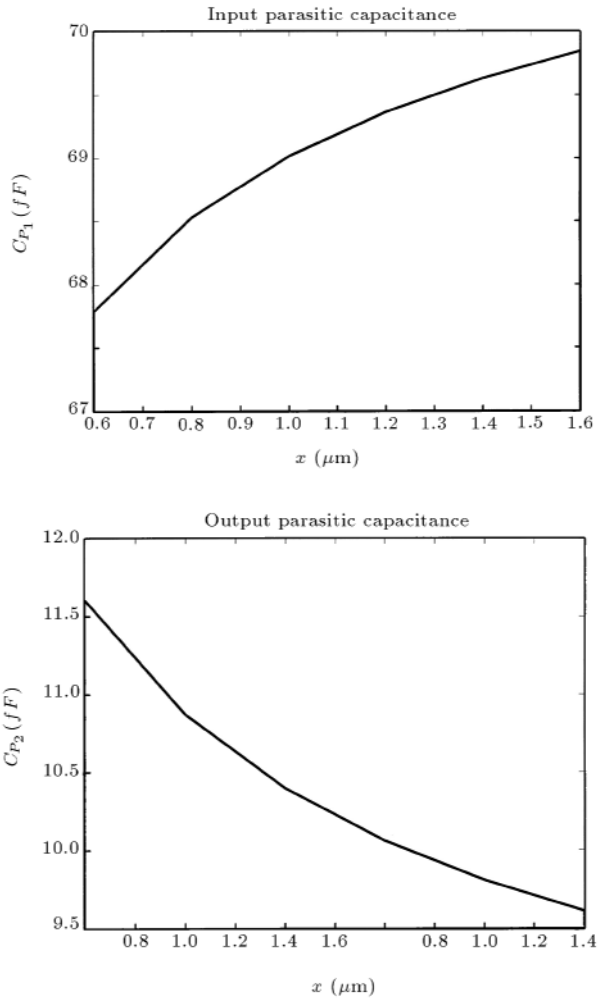

Figure 11. Simulated values of parasitic capacitances verses distance of two plates.

As a classic parallel plate capacitance, the variation of the capacitance, according to the inverse of the distance $(1/x)$, is assumed to be linear. Because of parasitic effects, e.g. fringing, the intrinsic capacitor has a 29.5 fF offset when $1/x$ tends to zero. Equation 13 is presented to describe the capacitance variation. The parameter extraction algorithm is realized by MATLAB 6.5 software from Mathworks.

$$C(fF) = 29.5 + \frac{310.9}{x}. \tag{13}$$

The resistance, R, is described as a quadratic function of the gap distance in the following equation:

$$R(K\Omega) = 16.6x^2 + 12.8x \quad 2.8. \tag{14}$$

In Figures 9 and 10, the values predicted by these behavioral models are compared with the simulation results of the structure. The figures show very good agreement between two sets of results. The model error is less than 0.25% for resistance and 0.57% for capacitance evaluating.

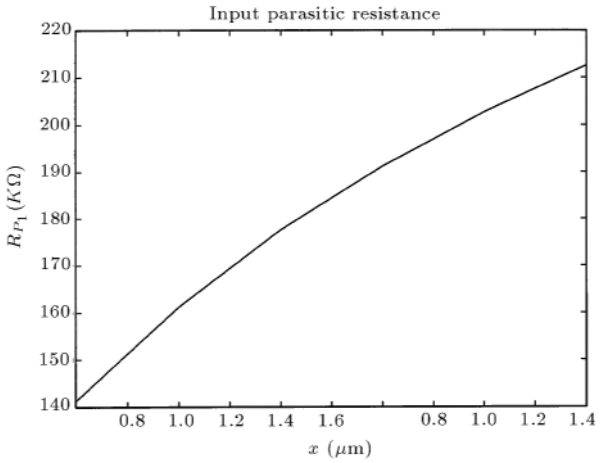

Figure 12. Simulated values of parasitic resistance.

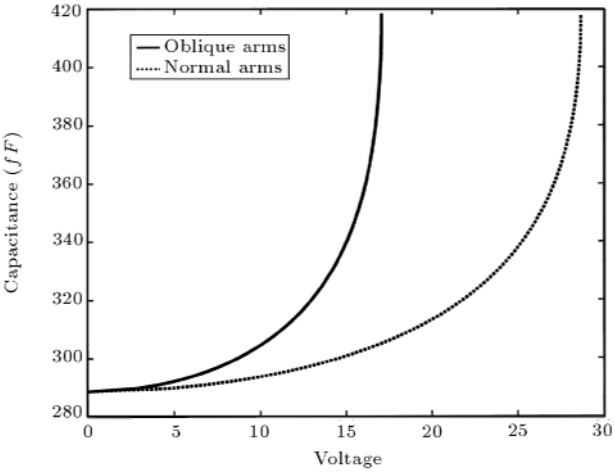

Figure 13. Variation of intrinsic capacitance versus bias voltage.

Figure 13 presents the variation of intrinsic capacitance versus applied bias voltage for both an oblique beam and a normal beam. As expected, the tuning range is limited by the pull-in effect, which is predicted to be about 146%, but, the effect of the oblique beams in decreasing the pull-in voltage, from 2.86 V to 1.7 V, is vividly obvious.

MODEL VERIFICATION

A scattering parameters prediction has been used for model verification. The equivalent circuit model is defined in APLAC, an object-oriented simulator and design tool, as a user defined model. The software was chosen because of its powerful RF module and simplicity [9].

The s-parameters are calculated at each gap distance for variable bias points. The result was compared with MEMS scattering parameters extracted from the EM simulation and shows good agreement between the two groups of parameters. The EM simulated

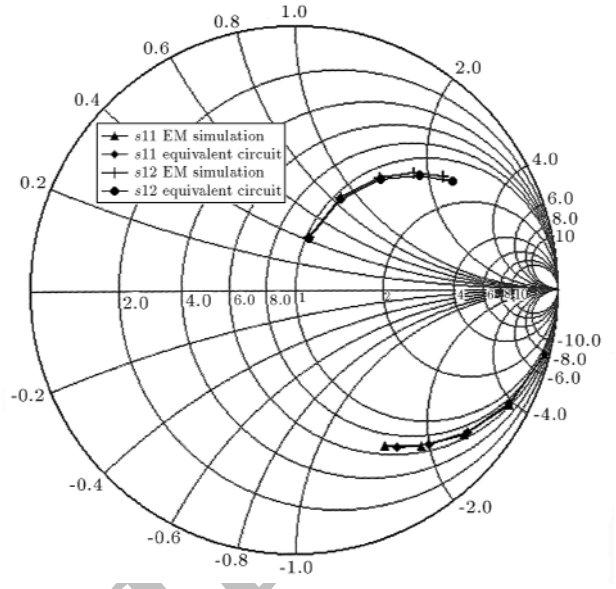

Figure 14. Comparison of scattering parameters.

and equivalent circuit parameters are presented on the Smith chart. Figure 14 shows the agreement between the parameters for a gap distance equal to 1 μm. The comparison between the two sets of scattering parameters was done by an error estimation algorithm. The results show that there is 2.6% and 2.9% error in determining s_{11} and s_{12} arguments and a 0.02 radian difference between the phases.

CONCLUSION

A new oblique suspender voltage tunable MEMS capacitor has been designed and electromagnetically simulated. Although the tuning range of the capacitance is limited by the pull-in effect, by using oblique arms, the beam deflection was increased and so, therefore, was the tunability of the capacitance. A behavioral intrinsic model and an equivalent circuit are extracted from EM simulations. The modeling error for all levels of modeling is less that 1%.

ACKNOWLEDGMENT

The authors wish to thank Professor Marco Farina from MEM Research for his guidance and for providing the EM3DS tool to carry out this work. The support of the Microelectronic Research Laboratory at the Ferdowsi University of Mashhad is also acknowledged.

REFERENCES

1. Nguyen, C.T. "Communication application of miroelectromechanical systems", *Proceedings, 1998 Sensors Expo.*, San Jose, CA, pp 447-455 (May 1998).
2. Katehi, L.P.B., Harvey, J.F. and Brown, E. "MEMS and Si micromachined circuits for high-frequency ap-

plications", *I IEEE Transaction on Microwave Theory and Techniques*, **50**(3), pp 858-866 (March 2002).

3. De Los Santos, H.J., *RF MEMS Circuit Design*, Artech House, Boston (2002).
4. Bushyager, N., Tentzeris, M.M., Gatewood, M.M. and DeNatale, L. "A novel adaptive approach to modeling MEMS tunable capacitors using MRTD and FDTD techniques", *Microwave Symposium Digest, 2001 IEEE MTT-S International*, **3**, pp 2003-2006 (20-25 May 2001).
5. Zou, J., Liu, C., Schutt-Aine, J., Chen, J. and Kang, S. "Development of a wide tuning range MEMS tunable capacitor for wireless communication systems", *Electron Devices Meeting, 2000, IEDM Technical Digest. International*, pp 403-406 (Dec. 2000).
6. Beer, F.P. and Johnston, E.R., *Mechanics of Materials*, McGraw Hill (1992).
7. *EM3DS 6.1 User Manual Release 1.5*, MEM Research (May 2003).
8. Farina, M. and Rozzi, T. "A 3-D integral equation-based approach to the analysis of real-life MICs-application to microelectromechanical systems", *IEEE Transaction on Microwave Theory and Techniques*, **49**(12) pp 2235-2240 (December 2001).
9. *APLAC 7.90 User Manual*, APLAC Solution Corporation (2003).